Dual-Band Metal-Only Antenna Combining Reflectarray and Reflector Functionalities

Zhihang An, Tony Makdissy, María Garcia Vigueras, Raphaël Gillard

Dual-Band Metal-Only Antenna Combining Reflectarray and Reflector Functionalities

Zhihang An[1], Tony Makdissy[2], María Garcia Vigueras[1], Raphaël Gillard[1]
[1] Institute of Electronics and Telecommunications of Rennes, INSA, 35708 Rennes, France, Zhihang.An@insa-rennes.fr
[2] TICKET Research Laboratory, Antonine University, 40016 Hadat-Baadba, Lebanon

***Abstract*—This paper presents a dual band metal-only antenna that operates at 20/40GHz. The proposed metal-only antenna combines the functionalities of reflectarray and parabolic reflector antennas. The unit cell consists of a square waveguide with short circuit termination and a square metallic block in the center. At 20GHz, the reflected beam is determined by a parabolic surface. At 40GHz, the reflected beam is controlled by the phase distribution of cells in the antenna. The gain increases with frequency in the lower frequency band, which is similar to what happens in a parabolic reflector antenna. The aperture efficiency at 20/40GHz is about 22.99/43.79%.**

***Index Terms*—metal-only, waveguide, reflectarray antenna.**

I. INTRODUCTION

Reflectarray antennas (RAs) can be seen as a combination of planar arrays and parabolic reflectors with the advantages of high gain, low profile, low cost and easy manufacturing. In some applications, RAs are required to operate in two different frequency bands. The dual band RAs are often achieved by using microstrip phase-shifting cells [1-13], where the reflection phases at both bands are tuned either by varying the geometry or using the variable rotation technique. In [14], an all-dielectric dual band RA is proposed where two different dielectric mirrors are used to control the reflection phase of the two frequency bands respectively. For all previously mentioned dual band RAs, a dielectric material is used, which makes of these solutions not suitable for some applications in severe environment, such as space. In such a situation, a metal-only (MO) RA is preferable as it avoids the intrinsic problems brought by the dielectric materials such as outgassing and temperature-dependent dielectric constant. A dual band MORA consisting of slot-type phoenix cell is thus proposed in [15]. This dual band MORA is synthesized by optimizing the total phase error at two frequency bands simultaneously.

Nevertheless, for all dual band RAs in [1-15], the main beams of both frequency bands are completely determined by the phase distributions over the RA cells. At the same time, they are of flat structure. This paper proposes a dual band MO antenna which combines the parabolic reflector and RA. For the sake of simplicity, it is referred to as reflector reflectarray antenna (RRA) in this paper. Nowadays the fabrication of such structures is possible thanks to the development of 3D printing technology. The proposed dual band MORRA is made of short-ended waveguides loaded by a central metal block. In the lower frequency band, the incident wave cannot propagate in the waveguide and is reflected back directly. The main beam is thus determined by the parabolic shape of the aperture. In this case, it corresponds to true-time delay with no bandwidth limitation. In the upper frequency band, the incident wave can propagate in the waveguide thanks to the metal loading and the main beam is collimated by varying the geometry of each cell. Note that the directions of the main beams are different in both frequency bands. Based on the principle of the proposed dual band MORRA, a very large frequency ratio between both bands can be achieved. As an example, a dual band MORRA operating at 20/40GHz is designed in this paper. Although a reflector antenna with similar principle has been reported in [16], the proposed MORRA in this paper is quite different from it. First, the used phase-shifting cell is different. In [16], the reflection phase at higher frequency is tuned only by a short-ended rectangular waveguide. Therefore the periodicity (after taking into account the cutoff frequency of TE_{10} mode) has to be greater than half a wavelength at higher frequency, which may result in grating lobes. The antenna in [16] also has a large side lobe level caused by the specular reflection which is suppressed in this paper. Finally, our structure is a fully metallic one, compatible with a simple additive manufacturing process.

This paper offers the detailed analysis and design of a dual band MORRA. Part II introduces the proposed concept for dual band MORRA. Part III presents the proposed unit cell. Part IV describes the design and simulation of the dual band MORRA. Finally, a conclusion is made in part V.

II. PROPOSED CONCEPT FOR DUAL BAND ANTENNA

Before the unit cell is introduced, the principle of dual band MORRA, as shown in Fig.1, is analyzed first. The proposed dual band RRA consists of short-ended metal waveguides. The waveguides are accommodated in such a way that their top surface approximately forms a paraboloid. If the frequency of the incident wave from the feed antenna is less than the cutoff frequency of these waveguides, the incident wave will be reflected back directly at the entrance of each waveguide. In this case, the incident wave is collimated only by the shape of the aperture and the operating mechanism is the same as the one of a parabolic reflector. If the frequency of the incident wave is greater than the cutoff frequency of the waveguides, the incident wave propagates inside and an additional phase shift is obtained which value depends on the length of each waveguide. As a result, a dual band MORRA can be designed. Once the shape of the aperture is determined in the lower frequency band, the reflected beam in the upper

frequency band is obtained thanks to the phase distribution produced by the unit cells of the RRA.

III. UNIT-CELL

In this paper, the unit cell is designed for operation at 20 and 40GHz. Based on the concept previously described, the reflection phase at 20GHz must be constant, and a complete 360° phase range is required at 40GHz. The unit cell consists of a short-ended waveguide loaded with a metallic block (see Fig.2). The proposed structure is a simplification of the 3D phoenix cell [17-18] which consists of two concentric square waveguides and a square metallic block in the center. The central metallic block allows to decrease the cut-off frequency of the quasi TE_{10} mode, thus to reduce the cell cross-section to prevent from grating lobes in the RRA. The detailed parameters of the proposed cell are tabulated in table I. The unit cell is simulated in HFSS®. The metal conductivity is set to 1.33×10^6 S/m (stainless) for the sake of realism. Floquet port is used and periodic boundary condition is assigned on the lateral faces to mimic a cell in a periodic infinite environment. The simulated reflection phase and loss under normal incidence at 20/40GHz are summarized in Fig.3. It can be seen that the range of variation of the reflection phase is less than 10° and the loss is negligible at 20GHz. The 360° phase range is achieved and the loss is less than 2 dB at 40GHz. These results show that the unit cell in Fig.2 can be used to design the dual band MORRA.

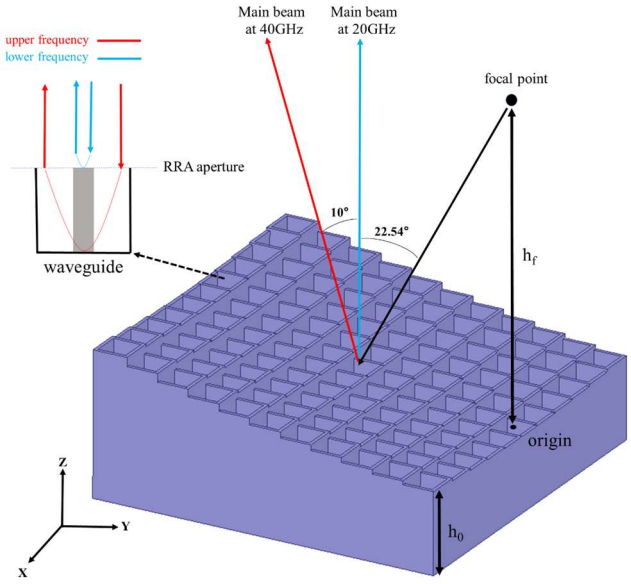

Fig.1. The principle and configuration of proposed dual band MORRA

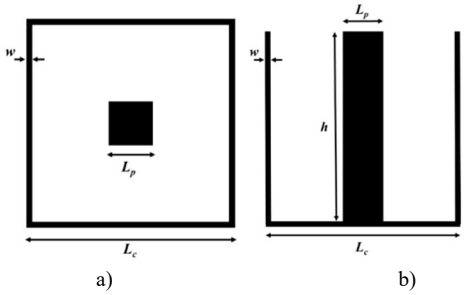

a) b)

Fig.2. The unit cell: a) top view, b) sectional view

TABLE I. THE DETAILED PARAMTERS OF UNIT CELL

Parameter	L_c	L_p	h	w
Value (mm)	3.75	1.5-2.5	5.5-7.8	0.2

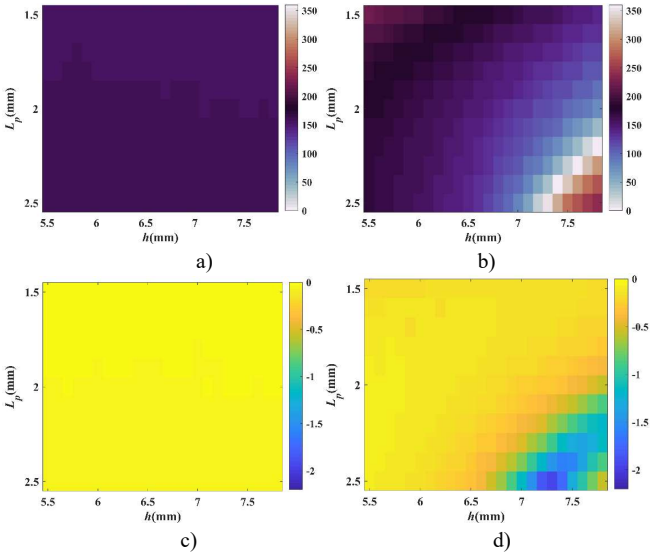

Fig.3. The reflection phase and the magnitude (normal incidence): a) phase at 20GHz (deg), b) phase at 40GHz (deg), c) magnitude at 20GHz (dB), d) magnitude at 40GHz (dB)

IV. ANTENNA DESIGN

In this section, the proposed dual band MORRA is designed. The design process is divided into 2 successive steps:

1) First, the position of the focal point and the shape of RRA surface are determined. This step is to make the RRA works as a parabolic reflector in the lower frequency band.

2) Next, the required phase shift of each cell is calculated based on the position of the feed phase center and the coordinates of each cell in the RRA. This allows generating, in the upper frequency band, a pencil beam in a different direction than that of the lower frequency band. A RRA can be synthesized by matching the required phase shift and the geometric parameters (h and L_p) of each cell.

The configuration of the dual band MORRA is shown in Fig.1. An offset configuration is used to avoid feed-blockage. The radiating aperture is D×D ($11.5\lambda_{up}\times11.5\lambda_{up}$, λ_{up} being the wavelength in free space at 40GHz) while the element spacing is $0.5\lambda_{up}$. A reserved space h_0 is used to tune the reflection phase. The position of focal point is set to (0, 0, h_f) where h_f is equal to 1.2D. The z coordinates of each cell (the center of the top surface of each cell) can be given by:

$$z_i = \frac{x_i^2+y_i^2}{4\times h_f} \quad (1)$$

where (x_i, y_i, z_i) represents the coordinates of each cell. The calculated z coordinates are summarized in Fig.4.

The proposed antenna configuration generates at the lower frequency band a pencil beam in the broadside direction owing to the presence of the parabolic surface. The direction of the main beam in the upper frequency band is set to (θ_0=10°, φ_0=270°) which is 10° away from the direction in the lower

frequency band (see Fig. 1). Then the required phase shift of the ith cell in the RRA at 40GHz can be calculated using the following equation:

$$\emptyset_{r\_i} = k(R_i - (x_i \sin\theta\cos\varphi + y_i \sin\theta \sin\varphi + z_i \cos\theta)) \quad (2)$$

where R_i is the distance between the phase center of the feed and the ith cell. (θ_0, φ_0) is the direction of main beam at 40GHz and k is the wave number in free space at 40GHz. Note that, unlike the case of planar RAs, the z coordinate of each cell is considered during the calculation of the required phase shift. The required phase of each cell is shown in Fig.5. It is a simple linear phase since the compensation of the different delays from feed horn is already compensated for by the parabolic shape.

The dual band RRA is illuminated with a feed antenna pointing to the cell in the center. The resulting incident angle in the center is 22.54°. Since the cells in the center have stronger illumination intensity, the database of the reflection phase provided by the cell is established for this particular incidence angle. The corresponding reflection phase and loss for TM excitation at 40GHz are shown in Fig.6.

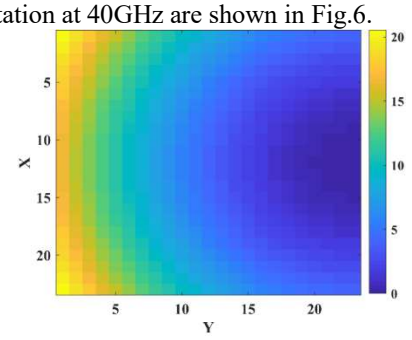

Fig.4. z coordinates of each cell

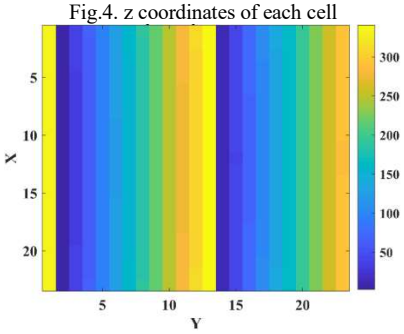

Fig.5. The distribution of the required phase shift

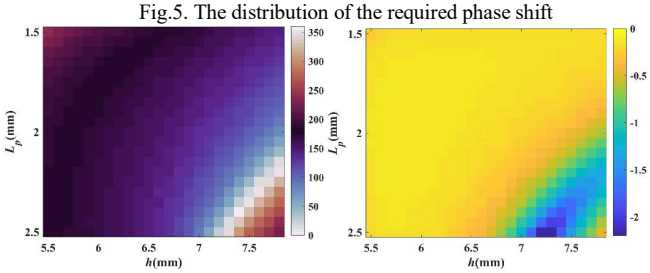

a) b)

Fig.6. The reflection phase and the magnitude at 40GHz (oblique incidence): a) reflection phase (deg), b) magnitude at 40GHz (dB)

The dual band RRA is synthesized by matching the required phase shift of each cell at 40GHz (Fig.5) and the database (Fig.6). The designed RRA with feed antenna is shown in Fig.7. In order to make a full wave simulation possible at the higher frequency, the dimensions in this preliminary design are chosen to be quite small (only $5.75\times5.75\lambda^2$ at 20GHz) and a simple rectangular waveguide is used to illuminate the antenna. A horn antenna is used for the upper frequency band. The simulation results in both frequency bands are summarized in Fig.8 and Fig.9. It can be seen that the main beam is in the broadside direction and the gain increases with frequency in the lower frequency band (as can be expected for a parabolic reflector). Also, the main beam in the upper frequency band points to the desired direction. The aperture efficiency at 20/40GHz is about 22.99/43.79%. The side lobe and cross polarization at 20/40GHz are below -11.45dB/-15.85dB and -27.37dB/-27.97dB respectively. These results demonstrate that the designed RRA can operate in two different frequency bands.

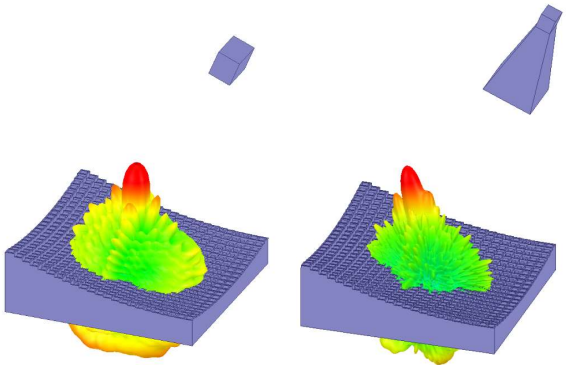

a) b)

Fig.7. The designed dual band MORRA with feed antenna: a) 20GHz, b) 40GHz

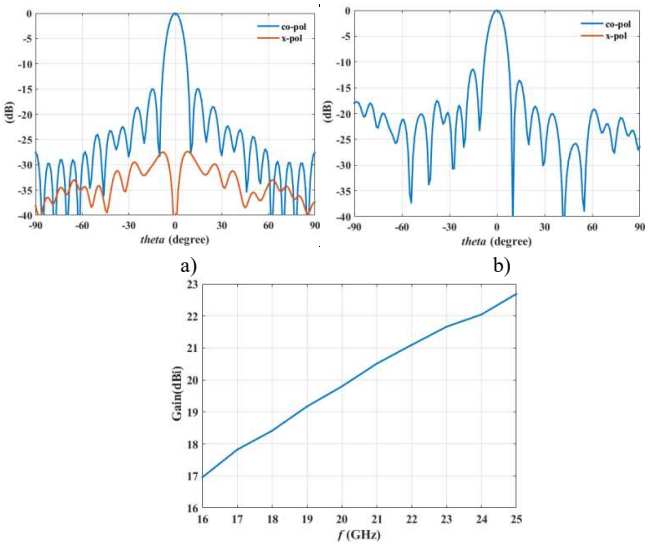

a) b)

c)

Fig.8. The simulation results in the lower frequency band: a) 20GHz xoz plane, b) 20GHz yoz plane, c) gain versus frequency

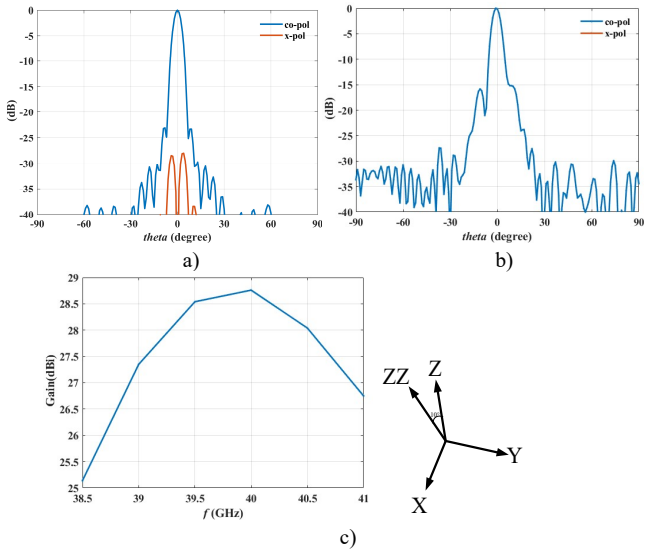

Fig.9. The simulation results in the upper frequency band: a) 40GHz xozz plane, b) 40GHz yozz plane, c) gain versus frequency

V. CONCLUSSION

In this work, an antenna combining reflectarray and reflector functionalities is proposed. This configuration allows to attain dual band operation. The considered structure is fully metallic. In the lower frequency band, the reflected beam is determined by the parabolic surface of the RRA. In the upper frequency band, the reflected beam is controlled by the phase distribution over the RRA cells. The simulation results show that the gain increases with frequency in the lower frequency band. Also, the aperture efficiency at 20/40GHz is about 22.99/43.79%.

ACKNOWLEDGMENT

The work was jointly funded by the Agence Universitaire de la Francophonie (Moyen-Orient), the National Council for Scientific Research Lebanon (CNRS-L) and China Scholarship Council (CSC).

REFERENCES

[1] Hsu S H, Han C, Huang J, et al. An offset linear-array-fed Ku/Ka dual-band reflectarray for planet cloud/precipitation radar[J]. IEEE transactions on antennas and propagation, 2007, 55(11): 3114-3122.

[2] You B Q, Liu Y X, Zhou J H, et al. Numerical synthesis of dual-band reflectarray antenna for optimum near-field radiation[J]. IEEE Antennas and Wireless Propagation Letters, 2012, 11: 760-762.

[3] Zhao J, Li T, Cui X, et al. A low-mutual coupling dual-band dual-reflectarray antenna with the potentiality of arbitrary polarizations[J]. IEEE Antennas and Wireless Propagation Letters, 2017, 16: 3224-3227.

[4] Smith T, Gothelf U, Kim O S, et al. Design, manufacturing, and testing of a 20/30-GHz dual-band circularly polarized reflectarray antenna[J]. IEEE Antennas and Wireless Propagation Letters, 2013, 12: 1480-1483

[5] Qu S W, Chen Q Y, Xia M Y, et al. Single-layer dual-band reflectarray with single linear polarization[J]. IEEE Transactions on Antennas and Propagation, 2013, 62(1): 199-205.

[6] Hamzavi-Zarghani Z, Atlasbaf Z. A new broadband single-layer dual-band reflectarray antenna in X-and Ku-bands[J]. IEEE Antennas and Wireless Propagation Letters, 2014, 14: 602-605.

[7] Deng R, Mao Y, Xu S, et al. A single-layer dual-band circularly polarized reflectarray with high aperture efficiency[J]. IEEE Transactions on Antennas and Propagation, 2015, 63(7): 3317-3320.

[8] Guo L, Tan P K, Chio T H. Single-layered broadband dual-band reflectarray with linear orthogonal polarizations[J]. IEEE Transactions on Antennas and Propagation, 2016, 64(9): 4064-4068.

[9] Deng R, Xu S, Yang F, et al. Single-layer dual-band reflectarray antennas with wide frequency ratios and high aperture efficiencies using phoenix elements[J]. IEEE Transactions on antennas and Propagation, 2016, 65(2): 612-622.

[10] Su T, Yi X, Wu B. X/Ku dual-band single-layer reflectarray antenna[J]. IEEE Antennas and Wireless Propagation Letters, 2019, 18(2): 338-342.

[11] Chen Y, Chen L, Wang H, et al. Dual-band crossed-dipole reflectarray with dual-band frequency selective surface[J]. IEEE Antennas and Wireless Propagation Letters, 2013, 12: 1157-1160.

[12] Xu P, Li L, Li R, et al. Dual-Circularly Polarized Spin-Decoupled Reflectarray With FSS-Back for Independent Operating at Ku-/Ka-Bands[J]. IEEE Transactions on Antennas and Propagation, 2021, 69(10): 7041-7046.

[13] Deng R, Yang F, Xu S, et al. An FSS-backed 20/30-GHz dual-band circularly polarized reflectarray with suppressed mutual coupling and enhanced performance[J]. IEEE Transactions on Antennas and Propagation, 2016, 65(2): 926-931.

[14] Zhu J, Yang Y, Mcgloin D, et al. 3-D Printed All-Dielectric Dual-Band Broadband Reflectarray With a Large Frequency Ratio[J]. IEEE Transactions on Antennas and Propagation, 2021, 69(10): 7035-7040.

[15] Deng R, Xu S, Yang F, et al. Design of a low-cost single-layer X/Ku dual-band metal-only reflectarray antenna[J]. IEEE Antennas and Wireless Propagation Letters, 2017, 16: 2106-2109.

[16] Chou H T, Lertwiriyaprapa T, Akkaraekthalin P, et al. Flexible dual-band dual-beam radiation of reflector antennas by embedding resonant phase alignment elements for power refocusing[J]. IEEE Transactions on Antennas and Propagation, 2020, 68(6): 4259-4270.

[17] Makdissy T, Gillard R, An Z, et al. Dual linearly polarised 3D printed Phoenix cell for wide band metal only reflectarrays[J]. IET Microwaves, Antennas & Propagation, 2020, 14(12): 1411-1416.

[18] An Z, Makdissy T, Vigueras M G, et al. A Metal-Only Reflectarray Made of 3D Phoenix Cells[C]//2022 16th European Conference on Antennas and Propagation (EuCAP). IEEE, 2022: 1-5.